

SYNTHESIS OF NEW PIROXICAM DERIVATIVES AND THEIR INFLUENCE ON LIPID BILAYERS

BERENIKA SZCZEŚNIAK-SIEGA^{1*}, JADWIGA MANIEWSKA¹, ANDRZEJ POŁA², KAMILA ŚRODA-POMIANEK², WIESŁAW MALINKA¹ and KRYSZYNA MICHALAK²

¹Department of Chemistry of Drugs, Wrocław Medical University,
Borowska 211, 50-556 Wrocław, Poland

²Department of Biophysics, Wrocław Medical University, Chałubińskiego 10, 50-368 Wrocław, Poland

Abstract: A novel series of potentially biologically active 1,2-benzothiazine 1,1-dioxides – analogs of piroxicam (a recognized non-steroidal anti-inflammatory drug) were synthesized from commercially available saccharin. All of the synthesized compounds were subjected to preliminary evaluation for their ability to interact with lipid bilayers. The influence of the new derivatives of piroxicam on liposomes made of EYPC was investigated by fluorescence spectroscopy with two fluorescent probes – Laurdan and Prodan. All the studied compounds showed an interaction with model membranes.

Keywords: synthesis, piroxicam, lipid bilayers, fluorescence spectroscopy, multitarget drugs, benzothiazines, MDR

The discovery of drugs these days is based upon a “one molecule – one target – one disease” philosophy, but modulating multiple protein targets simultaneously can be more beneficial for treating complex diseases, for instance, cancer, diabetes or neurodegenerative diseases like Alzheimer’s disease (1). Our understanding of systems biology and the molecular complexity of human diseases has substantially shifted current therapeutic thinking towards drugs acting upon many molecular targets, i.e., multitarget drugs. Moreover, to fully understand the actions of a drug, knowledge of its polypharmacology is clearly essential (2, 3).

Since it is becoming well understood that chronic inflammation in any form can initiate and accelerate the cancer process, NSAIDs (non-steroidal anti-inflammatory drugs), which inhibit inflammation, became anti-cancer drugs (4, 5). The molecular target of NSAIDs is cyclooxygenase (COX), the enzyme which catalyzes the conversion from arachidonic acid to prostaglandins (PGs). There are three isoforms of COX (COX-1, COX-2 and COX-3) (6). The inhibition of COX-2 is responsible for the decrease in colorectal, breast, prostate and lung cancer incidence. That is why NSAIDs have been reported to reduce the risk of some solid tumors and are one of the most promising chemo-

preventive agents for cancer. Among the many NSAIDs studied as chemopreventive agents, there is a distinguished group of *oxicams* (e.g. piroxicam, meloxicam, tenoxicam), identified by their benzene(thieno)thiazine heterocyclic system containing an enolic group in position 4 (7).

Lichtenberger et al. presume that one of the alternative mechanisms by which NSAIDs can be effective is by interacting with cellular membranes and altering their biophysical properties (8). What is more, Peetla et al. prove that biophysical changes in membrane lipids in multidrug resistance (MDR) of cancer cells influence the transport and delivery of anticancer drugs. Recent advances in membrane lipid research show the varied roles of lipids in regulating membrane P-glycoprotein (P-gp) function, membrane trafficking, apoptotic pathways, drug transport and endocytic functions. Therefore, understanding the relationship between biophysical aspects of the cell membrane in drug-resistance mechanisms and drug delivery processes is crucial to overcome the phenomenon of MDR (9). It is proved that a lipid bilayer’s composition and fluidity affect P-gp function, which efflux system occurs in drug-resistant cancer cells (10).

We designed new piroxicam (4-hydroxy-2-methyl-N-(pyridin-2-yl)-2H-1,2-benzothiazine-3-

* Corresponding author: berenika.szczesniak-siega@umed.wroc.pl

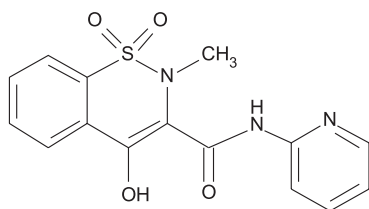


Figure 1. Structure of piroxicam

carboxamide 1,1-dioxide), (Fig. 1) derivatives as potentially multitarget drugs. They would be an analgesic, anti-inflammatory and, at the same time, chemopreventive in cancer. And, what is more, it might be the modulator overcoming the MDR phenomenon in resistant cancer cells. In our present work, we describe the procedure of synthesis of four new piroxicam derivatives, named **PD 28–31** (Fig. 2), and the results of studies of the interaction of new compounds with lipid bilayers by means of fluorescence spectroscopic methods. Also molecular structures of all compounds were optimized by molecular mechanics calculations *in silico*.

EXPERIMENTAL

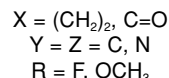
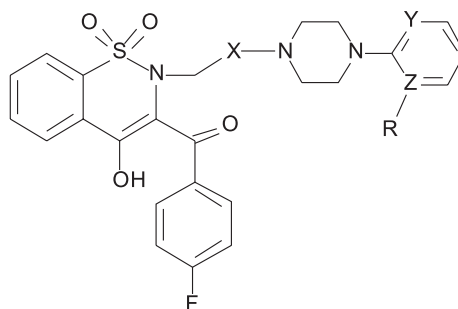
Chemicals

The reagents and solvents used for synthesis were purchased from commercial suppliers and used as received. Homogeneity of the compounds was checked by TLC on silica gel plates. Flash column chromatographic purifications were performed using Sigma-Aldrich 60A silica gel 230–400 mesh. The proton nuclear magnetic resonance (¹H-NMR) spectra were measured on a Bruker 300 MHz NMR spectrometer using CDCl₃ as solvent and TMS as an internal standard. Melting points were determined in open capillary tubes and are uncorrected. Elemental analyses were performed with Carlo Erba NA 1500 analyzer and were within ± 0.4% of the theoretical value. IR spectra (cm⁻¹) were recorded on a Perkin-Elmer Spectrum Two UATR FT-IR spectrometer. The samples were applied as neat solids.

Phospholipid: egg yolk phosphatidylcholine (EYPC) was purchased from Sigma-Aldrich (Poznań, Poland). The lipid was used as delivered, without further purification.

Fluorescent labels: 6-dodecanoyl-2-dimethylaminonaphthalene (Laurdan) and 6-propionyl-2-dimethylaminonaphthalene (Prodan) were purchased from Molecular Probes (USA).

All other chemicals used in this study were of analytical grade.

Figure 2. Structures of new piroxicam analogues – **PD 28–31**

General procedure for the preparation of **PD 28–31**

2-(4-Fluorophenacyl)-2H-1,2-benzothiazol-3-one 1,1-dioxide (**2**)

A mixture of commercially available saccharine **1** (0.92 g, 5 mmol) with 5 mmol of 2-bromo-4'-fluoroacetophenone in 7 mL of *N,N*-dimethylformamide (DMF) and triethylamine (0.7 mL, 5 mmol) was stirred at room temperature for 10 h, then poured over ice cooled water (50 mL) resulting in the formation of a white solid, which was filtered and washed with cold water. The solid was dried and crystallized from ethanol to give **2**.

Analytical data for **2**: C₁₅H₁₀FNO₄S (m.w. 319.31); m.p. 165–168°C (EtOH). ¹H-NMR (δ, ppm): 5.11 s (2H, CH₂), 7.16–8.01 m (8H, ArH). FT-IR (UATR): 1738, 1693 (CO), 1330, 1183 (SO₂) cm⁻¹. Yield 94%.

3-(4-Fluorobenzoyl)-4-hydroxy-2H-1,2-benzothiazine 1,1-dioxide (**3**)

Three millimole of **2** was dissolved in 7.5 mL of EtONa (prepared from 0.17 g of Na and 7.5 mL of anhydrous EtOH) at 40°C and stirred with heating to 55–60°C for 5–10 min. Color changes from beige to deep red were observed. After this time and after dissolving all of the substance, the mixture was rapidly cooled to 25°C and 7.5 mL HCl (9%) was added. Color changed from deep red to deep yellow and the product precipitated. The solid was filtered off, washed with cold water, dried and purified by crystallization from EtOH to give **3**.

Analytical data for **3**: C₁₅H₁₀FNO₄S (m.w. 319.31); m.p. 193–195°C (EtOH). ¹H-NMR (δ, ppm): 5.91 s (1H, NH), 7.13–8.20 m (8H, ArH), 15.80 s (1H, OH_{enolic}). FT-IR (UATR): 3151 (NH), 1590 (CO), 1280, 1158 (SO₂) cm⁻¹. Yield 81%.

1-(2-Chloro-1-oxoethyl)-4-arylsubstituted-piperazine (4a, b)

Ten millimoles of 1-(2-fluorophenyl)piperazine (for **4a**) or 1-(2-pyrimidin)piperazine (for **4b**) was dissolved in 40 mL of diethyl ether with addition of 1.4 mL of triethylamine and stirred slowly at room temperature for 10 min. Then, 1.6 mL (20 mmol) of chloroacetyl chloride in 20 mL of diethyl ether were slowly instilled, and stirring was continued for another 2 h. After this time, diethyl ether was evaporated in vacuum and 10 mL of water and 60 mL of chloroform were added. The organic phase was separated, dried with MgSO_4 and evaporated in vacuum to give **4a** or **4b**.

Analytical data for **4a**: $\text{C}_{12}\text{H}_{14}\text{ClFN}_2\text{O}$ (m.w. 256.70); $^1\text{H-NMR}$ (CDCl_3 , δ , ppm): 3.02–3.12 (m, 4H, $\text{N}(\text{CH}_2)_2$), 3.64–3.78 (m, 4H, $\text{N}(\text{CH}_2)_2$), 4.08 (s, 2H, CH_2), 6.87–7.06 (m, 4H, ArH). Yield 70%.

Analytical data for **4b**: $\text{C}_{10}\text{H}_{13}\text{ClN}_4\text{O}$ (m.w. 240.69); $^1\text{H-NMR}$ (CDCl_3 , δ , ppm): 3.56–3.70 (m, 4H, $\text{N}(\text{CH}_2)_2$), 3.82–3.92 (m, 4H, $\text{N}(\text{CH}_2)_2$), 4.11 (s, 2H, CH_2), 6.53–6.56 [t, $J = 4.8$ Hz, 1H, $\text{CH}(5)_{\text{pyrimidine}}$], 8.31–8.33 [d, $J = 4.8$ Hz, 2H, $\text{CH}(4$ and $6)_{\text{pyrimidine}}$]. Yield 66%.

1-(3-Chloropropyl)-4-(2-substituted-phenyl)piperazine (5a, b)

Ten millimoles of 1-(2-fluorophenyl)piperazine (for **5a**) or 1-(2-methoxyphenyl)piperazine (for **5b**) and 11 mmol (1.1 mL) of 1-bromo-3-chloropropane were dissolved in acetone (3 mL) with addition of 25% NaOH (2 mL), stirred slowly at room temperature for 8 h and left overnight. After this time, ether (20 mL) was added and stirred for further 30 min. Then, the mixture was divided in a

separatory funnel into two parts. The ether part was dried with MgSO_4 and evaporated under vacuum. The residue was purified by flash silica gel chromatography, eluting with EtOAc to give **5a** or **5b**.

Analytical data for **5a**: $\text{C}_{13}\text{H}_{18}\text{ClFN}_2$ (m.w. 256.75); $^1\text{H-NMR}$ (δ , ppm): 1.96–2.05 (m, 2H, $\text{CH}_2\text{CH}_2\text{CH}_2$), 2.56–2.68 (m, 6H, $\text{CH}_2\text{N}(\text{CH}_2)_2$), 3.11–3.14 (m, 4H, $\text{N}(\text{CH}_2)_2$), 3.61–3.65 (t, $J = 6.6$ Hz, 2H, $\text{CH}_2\text{CH}_2\text{CH}_2\text{N}_{\text{piperazine}}$), 6.92–7.26 (m, 4H, ArH). Yield 85%.

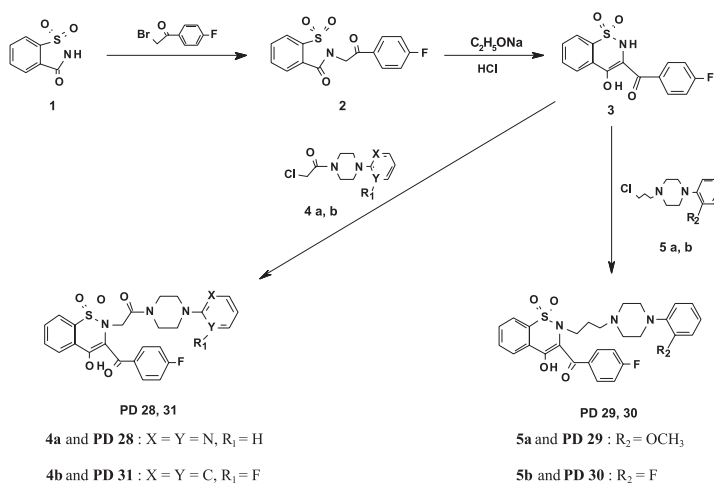
Analytical data for **5b**: $\text{C}_{14}\text{H}_{21}\text{ClN}_2\text{O}$ (m.w. 268.78); $^1\text{H-NMR}$ (δ , ppm): 1.94–2.04 (m, 2H, $\text{CH}_2\text{CH}_2\text{CH}_2$), 2.49–2.66 (m, 6H, $\text{CH}_2\text{N}(\text{CH}_2)_2$), 3.09 (brs, 4H, $\text{N}(\text{CH}_2)_2$), 3.59–3.63 (t, $J = 6.6$ Hz, 2H, $\text{CH}_2\text{CH}_2\text{CH}_2\text{N}_{\text{piperazine}}$), 3.85 (s, 3H, OCH_3), 6.83–7.02 (m, 4H, ArH). Yield 74%.

3-(4-Fluorobenzoyl)-2-substituted-4-hydroxy-2H-1,2-benzothiazine 1,1-dioxides (PD 28–31)

To the stirred mixture of 5 mmol **3** in 20 mL of anhydrous EtOH 5 mL of EtONa (prepared from 0.12 g of Na and 5 ml of anhydrous EtOH) was added. Then, 5 mmol of corresponding piperazine (**4a, b** or **5a, b**) was added and refluxed with stirring for 10–12 h. When the reaction was complete, which was confirmed on TLC plates, ethanol was distilled off, the residue was treated with 50 mL of CHCl_3 and insoluble materials were filtered off. The filtrate was evaporated and the residue was purified by crystallization from ethanol to give compounds **PD 28–31**.

Analytical data for **PD 28–31**:

PD 28: $\text{C}_{27}\text{H}_{23}\text{F}_2\text{N}_3\text{O}_5\text{S}$ (m.w. 539.55); m.p. 165–166°C (EtOH). $^1\text{H-NMR}$ (δ , ppm): 2.80–4.23 (m, 10H, CH_2CO and $\text{H}_{\text{piperazine}}$), 6.79–8.25 (m, 12H,



Scheme 1. General procedure for preparation of **PD 28–31**

ArH), 15.49 (s, 1H, OH_{enolic}). FT-IR (UATR): 1644, 1591 (CO), 1336, 1175 (SO₂) cm⁻¹. Analysis: calcd.: C 60.10, H 4.30, N 7.79%; found: C 59.97, H 4.40, N 7.59%. Yield 45%.

PD 29: C₂₅H₂₂FN₅O₅S (m.w. 523.54); m.p. 210–213°C (EtOH). ¹H-NMR (δ, ppm): 3.13–4.31 (m, 10H, CH₂CO and H_{piperazine}), 6.51–8.29 (m, 11H, ArH), 15.50 (s, 1H, OH_{enolic}). FT-IR (UATR): 1660, 1586 (CO), 1344, 1175 (SO₂) cm⁻¹. Analysis: calcd.: C 57.35, H 4.24, N 13.38%; found: C 57.39, H 4.28, N 13.46%. Yield 44%.

PD 30: C₂₈H₂₇F₂N₃O₄S (m.w. 539.59); m.p. 145–148°C (EtOH). ¹H-NMR (δ, ppm): 1.24 (brs, 2H, CH₂CH₂CH₂), 1.99 (brs, 2H, CH₂CH₂CH₂N_{piperazine}), 2.28 (brs, 4H, N(CH₂)₂), 2.95–3.42 (m, 6H, CH₂N(CH₂)₂), 6.91–8.19 (m, 12H, ArH), 15.50 (s, 1H, OH_{enolic}). FT-IR (UATR): 1607 (CO), 1331, 1174 (SO₂) cm⁻¹. Analysis: calcd.: C 62.32, H 5.04, N 7.79%; found: C 62.67, H 5.37, N 7.51%. Yield 55%.

PD 31: C₂₉H₃₀FN₃O₅S (m.w. 551.63); m.p. 121–123°C (EtOH). ¹H-NMR (δ, ppm): 1.39 (brs, 2H, CH₂CH₂CH₂), 2.10 (brs, 2H, CH₂CH₂CH₂N_{piperazine}),

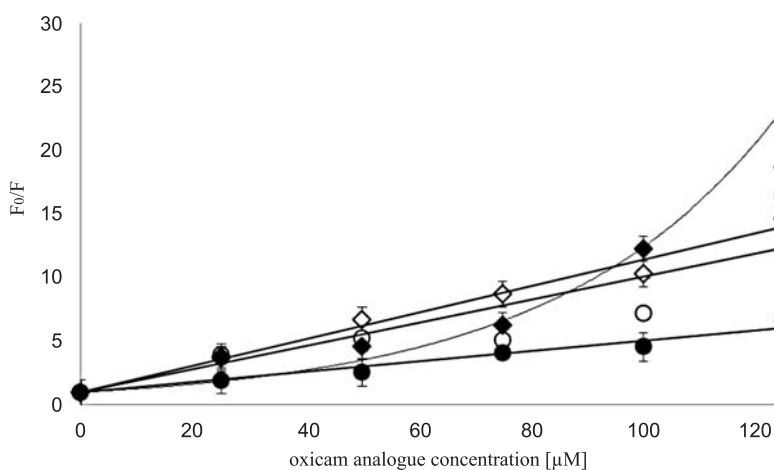


Figure 3. Stern-Volmer plots for quenching of Laurdan (open symbols) and Prodan (full symbols) by PD28 (circles) and PD29 (diamonds) in EYPC. Bars represent standard deviations

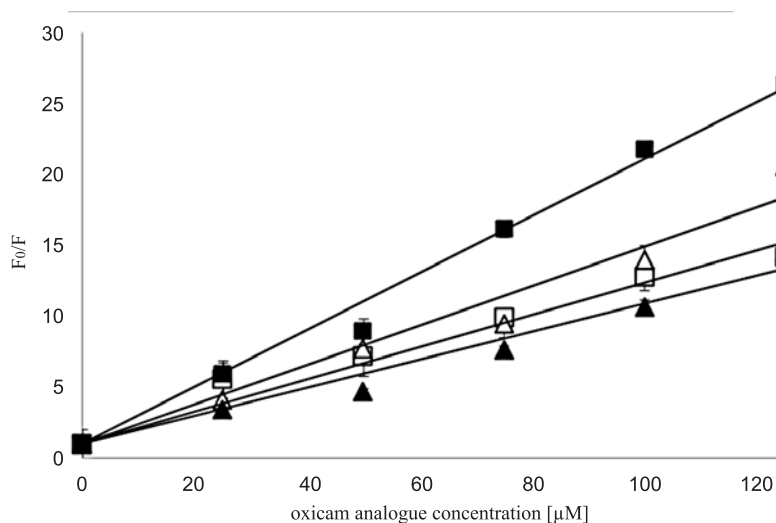


Figure 4. Stern-Volmer plots for quenching of Laurdan (open symbols) and Prodan (full symbols) by PD30 (squares) and PD31 (triangles) in EYPC. Bars represent standard deviations

2.44 (brs, 4H, N(CH₂)₂), 3.03–3.40 (m, 6H, CH₂N(CH₂)₂), 3.84 (s, 3H, OCH₃), 6.84–8.18 (m, 12H, ArH), 15.48 (s, 1H, OH_{enolic}). FT-IR (UATR): 1614 (CO), 1329, 1175 (SO₂) cm⁻¹. Analysis: calcd.: C 63.14, H 5.48, N 7.62%; found: C 63.36, H 5.63, N 7.54%. Yield 42%.

Fluorescence spectroscopy

Small unilamellar liposomes, prepared by sonification of 2 mM EYPC suspension in 20 mM Tris–HCl buffer (20 mM Tris, 0.5 mM EDTA, 150 mM NaCl pH 7.4) using UP 200s sonicator (Dr. Hilscher GmbH, Berlin, Germany), were used for fluorescence spectroscopy measurements. Final phospholipid concentration in a sample was 200 μM. Laurdan and Prodan were dissolved in DMSO in order to obtain 1 mM stock solutions. Liposomes were incubated with a fluorescent probe (final concentration 5 μM) for 30 min in darkness at room temperature. Then, the appropriate amount of oxamicam stock solution (30 mM DMSO) was added and the sample was further incubated for 20 min in darkness. The oxamicam concentration in samples was 25–125 μM in concentration-dependence experiments. All spectroscopic experiments were carried out at room temperature with LS 50B spectrofluorimeter (Perkin–Elmer Ltd., Beaconsfield, UK) equipped with a xenon lamp using emission and excitation slits of 5 nm. The excitation wavelength for Laurdan was 390 nm and for Prodan 360 nm. The recorded fluorescence spectra were processed with FLDM Perkin-Elmer 2000 software.

It was checked that the studied oxamicam analogues alone did not exhibit fluorescence in the spectral region of interest. All the experiments were performed three times.

Molecular modelling

Theoretical calculations were performed using Spartan 10 software (Wavefunction, Inc., USA). The optimized molecular structure of all compounds and QSAR (quantitative structure–activity relationship) descriptors for them were calculated *ab initio* by DFT method with 6-31+G* basis set.

RESULTS

Synthesis

Compound **2** was obtained by alkylation of saccharin with 2-bromo-4'-fluoroacetophenone in DMF with addition of a small amount of triethylamine in room temperature. Then, newly obtained compound was rearranged using sodium ethoxide to give compound **3**. The alkylation of **3** by

1-(chloroalkil/acyl)-4-arylpiperazine resulted in products **PD 28–31**.

Fluorescence spectroscopy

Laurdan and Prodan, two fluorescent probes, were used to characterize the interaction of the studied compounds with EYPC liposomes. Both probes possess the same fluorophore but connected to the propionyl chain in case of Prodan and to the lauryl chain in Laurdan (11). Laurdan fluorophore is located deeper in the lipid bilayer at the level of the phospholipid glycerol backbone, whereas Prodan, in contrast, is anchored to the lipid bilayer more loosely and resides closer to the membrane surface. In the studies it was initially checked if the addition of any of the studied compounds would result in fluorescence quenching of the probes. Stern–Volmer plots are presented in Figure 3 for **PD 28** and **PD 29** and in Figure 4 for **PD 30** and **PD 31**. The studied compounds caused very strong quenching of both probes, although the effect was much more pronounced in case of Laurdan for **PD 28** and **PD 31**, and in case of Prodan for **PD 29** and **PD 30**.

Molecular modelling

Applying of QSAR methods allowed to describe electronic, structural and topological parameters and hydrophobicity of new compounds and to correlate these properties with their ability to interact with model membranes. LogP of studied oxamicam derivatives is ranked as follows: **PD 30** > **PD 29** > **PD 31** > **PD 28** and PSA: **PD 28** > **PD 31** > **PD 29** > **PD 30**, while polarizability is ranked as follows: **PD 29** > **PD 30** > **PD 31** > **PD 28**. Values of all molecular descriptors for newly synthesized oxamicam derivatives are presented in Table 1.

Presented results revealed that newly synthesized compounds pass the Lipinski's Rule of five (RO5), because LogP < 5, H-bond donors < 5, and H-bond acceptors < 10 (12). These physicochemical parameters are associated with acceptable aqueous solubility and intestinal permeability so comprise the first steps in oral bioavailability and ability to interact with lipid bilayers.

DISCUSSION AND CONCLUSION

Our group has focused on synthesis of new chemical analogues of piroxicam with potential analgesic, anti-inflammatory and chemopreventive or anti-MDR activity as multitarget drugs. In the present work, we have shown that new compounds **PD 28–31** interact with the model membranes under consideration. Quenching of fluorescence of two probes, Laurdan and

Table 1. The molecular descriptors for **PD 28–31** (Spartan 10).

Compound	Log P	PSA [Å ²]	HBD Count	HBA Count	E HOMO [eV]	E LUMO [eV]	Polarizability
PD 28	0.32	91.799	1	10	-6.04	-2.65	79.47
PD 29	2.73	75.592	1	9	-5.79	-2.57	84.08
PD 30	3.02	70.503	1	8	-6.00	-2.54	82.20
PD 31	1.83	80.632	1	9	-5.95	-2.61	80.88

PSA = polar surface area, HBD = hydrogen bond donor, HBA = hydrogen bond acceptor, E HOMO = energy of highest occupied molecular orbital, E LUMO = energy of lowest unoccupied molecular orbital

Prodan, by four newly synthesized oxicam derivatives (**PD 28–31**) was investigated. According to Lakowicz, the extent of quenching expressed by the values of Stern-Volmer constants can reveal the accessibility of fluorophores to quenchers. That is why, if the location of fluorescent probe (fluorophore) within the model membranes is known, quenching studies can be used to reveal the location of quenchers in membranes or the permeability of membrane to quenchers (13). It was found that **PD 28** and **PD 31** quenched the fluorescence of Laurdan to a higher extent than Prodan in model membranes. On the contrary, **PD 29** and **PD 30** turned out to be weaker quenchers of Laurdan than Prodan fluorescence. The decreased fluorescence intensity in the presence of the studied compounds may be the result of their interaction with fluorescent probes affecting e.g., their influence on fluorophore's microenvironment or their molecular organization within the phospholipid bilayer. The more pronounced quenching of Laurdan than Prodan fluorescence for **PD 28** and **PD 31** in comparison to **PD 29** and **PD 30** suggested that the bilayer region occupied by Laurdan (the level of the phospholipid glycerol backbone) is more affected by their presence. The regions close to the surface of the model membrane, where Prodan is localized, were more affected by the presence of **PD 29** and **PD 30**. Quenching of the fluorescence of another fluorescent probe -DPH by NSAIDs (two oxicams - lornoxicam and meloxicam - and nimesulide) was examined by Sousa et al. (14). Their DPH fluorescence quenching studies revealed that studied NSAIDs were able to quench the fluorescence of the probe located in phospholipid bilayer hydrocarbon region - even deeper than Laurdan. Their fluorescence anisotropy measurements were also made to investigate the effects on membrane fluidity resulting from the interaction between the drugs and lipid bilayers. The efficiency of NSAIDs to increase the membrane fluidity and to penetrate into the hydrocarbon chain region was ordered as: lornoxicam > meloxicam > nimesulide. The deeper penetration of **PD 28** and **PD 31** into the lipid bilayer, revealed in our studies, may be related to the presence of

the additional carbonyl group in the side chain in position 2 of benzothiazine ring, which might increase their ability to interact with model membranes. However, the precise determination of the nature of new oxicam analogues interaction with phospholipid membranes would require further studies.

REFERENCES

- Morphy R., Rankovic Z.: *Drug Discov. Today* 12, 156 (2007).
- Hopkins A.L.: *Nature* 12, 462 (2009).
- Bojanowski P., Lipiński P., Czekąła P., Plewczyński D.: *Biul. Wydz. Farm. WUM* 1, 1 (2013) (Polish).
- Steele V.E., Hawk E.T., Viner J.L., Lubet R.A.: *Mutat. Res.* 523, 137 (2003).
- Grivennikov S., Greten F., Karin M.: *Cell* 19, 883 (2010).
- Sobolewski C., Cerella C., Dicato M., Ghibelli L., Diederich M.: *Int. J. Cell Biol.* 2010, 215158 (2010).
- Wang D., DuBois R.N.: *Nature Rev. Cancer* 10, 181 (2010).
- Lichtenberger L.M., Zhou Y., Jayaraman V., Doyen J.R., O'Neil R.G., Dial E.J., Volk D.E. et al.: *Biochim. Biophys. Acta* 1821, 994 (2012).
- Bamburowicz-Klimkowska M., Szutowski M.: *Biul. Wydz. Farm. WUM* 1, 1 (2012).
- Peetla Ch., Vijayaraghavalu S., Labhasetwar V.: *Adv. Drug Deliv. Rev.* 65, 1686 (2013).
- Parasassi T., Krasnowska E.K., Bagatolli L., Gratton E.: *J. Fluoresc.* 8, 4 (1998).
- Lipinski Ch., *Drug Discov. Today Technol.* 1, 337 (2004).
- Lakowicz J.R.: *Principles of Fluorescence Spectroscopy*. 3rd edn., Springer, Heidelberg, New York 2006.
- Sousa C., Nunes C., Lúcio M., Ferreira H., Lima J.L.F.C., Tavares J., Cordeiro-da-Silva A., Reis S.: *J. Pharm. Sci.* 97, 8 (2008).